Front. Chem. Sci. Eng. 2023, 17(4): 425–436
https://doi.org/10.1007/s11705-022-2229-0

RESEARCH ARTICLE

Efficient acetoin production from pyruvate by engineered *Halomonas bluephagenesis* whole-cell biocatalysis

Meiyu Zheng[1,2*], Zhenzhen Cui[1,2*], Jing Zhang[1,2], Jing Fu[3], Zhiwen Wang[1,2], Tao Chen (✉)[1,2]

1 Department of Biochemical Engineering, School of Chemical Engineering and Technology, Tianjin University, Tianjin 300350, China
2 Frontier Science Center for Synthetic Biology and Key Laboratory of Systems Bioengineering (Ministry of Education), School of Chemical Engineering and Technology, Tianjin University, Tianjin 300350, China
3 Department of Biology and Biological Engineering, Chalmers University of Technology, Gothenburg 41296, Sweden

Abstract Acetoin is an important platform chemical, which has a wide range of applications in many industries. *Halomonas bluephagenesis*, a chassis for next generation of industrial biotechnology, has advantages of fast growth and high tolerance to organic acid salts and alkaline environment. Here, *α*-acetolactate synthase and *α*-acetolactate decarboxylase from *Bacillus subtilis* 168 were co-expressed in *H. bluephagenesis* to produce acetoin from pyruvate. After reaction condition optimization and further increase of *α*-acetolactate decarboxylase expression, acetoin production and yield were significantly enhanced to 223.4 mmol·L^{-1} and 0.491 mol·mol^{-1} from 125.4 mmol·L^{-1} and 0.333 mol·mol^{-1}, respectively. Finally, the highest titer of 974.3 mmol·L^{-1} (85.84 g·L^{-1}) of acetoin was accumulated from 2143.4 mmol·L^{-1} (188.6 g·L^{-1}) of pyruvic acid within 8 h in fed-batch bioconversion under optimal reaction conditions. Moreover, the reusability of the cell catalysis was also tested, and the result illustrated that the whole-cell catalysis obtained 433.3, 440.2, 379.0, 442.8 and 339.4 mmol·L^{-1} (38.2, 38.8, 33.4, 39.0 and 29.9 g·L^{-1}) acetoin in five repeated cycles under the same conditions. This work therefore provided an efficient *H. bluephagenesis* whole-cell catalysis with a broad development prospect in biosynthesis of acetoin.

Keywords acetoin, pyruvate, *α*-acetolactate synthetase, *α*-acetolactate decarboxylase, *Halomonas bluephagenesis*, whole-cell biocatalysis

1 Introduction

Acetoin, also known as 3-hydroxybutanone, methyl acetyl methanol, is naturally existed in dairy products and some fruits with a special milk flavor, and is widely used in food, pharmaceuticals, chemical and other industries [1–3]. In 2004, it was listed as one of the 30 platform compounds for priority development and utilization by the Department of Energy of the United States [4,5]. Biological production of acetoin exhibits better potential compared with traditional chemical synthesis, such as higher product safety and less pollution to the environment [3,6,7]. There are widely reported three strategies for biological acetoin production, which are microbial fermentation, *in vitro* enzyme biocatalysis, whole-cell biocatalysis [6]. A range of native and recombined microorganisms had been proved to produce acetoin efficiently, including *Bacillus subtilis* [8], *Serratia marcescens* [4], *Saccharomyces cerevisiae* [9], *Escherichia coli* [5], etc. According to the reports on acetoin production by microbial fermentation, a titer of 102.5 g·L^{-1} acetoin was obtained from glucose with a yield of 0.419 g·g^{-1} by a fed-batch strategy in 5 L bioreactor using engineered *Corynebacterium glutamicum* [10]. Besides, Bae et al. [11] obtained 101.3 g·L^{-1} of (*R*)-acetoin with high yield from glucose in rich yeast peptone dextrose medium by engineered *S. cerevisiae*. Glycerol was also used for acetoin production. Almuharef et al. [12] used the strain SRWQ1 to produce a significant amount of acetoin (8.38 ± 0.76 g·L^{-1}) with a yield of 0.06 g·g^{-1} from glycerol. A wide range of substrates and host bacteria were used in microbial fermentation for acetoin production but the titer of acetoin was hard to further elevate after it reached 100 g·L^{-1}. As for *in vitro* enzyme biocatalysis, it had a complex enzyme extraction and purification process, which greatly increased the complexity and cost of the bioconversion process, thus this method was not much conducive to industrial application. Compared with these two approaches, whole-cell biocatalysis had the advantages of eliminating the

Received April 23, 2022; accepted July 28, 2022

E-mail: chentao@tju.edu.cn

* These authors contributed equally to this work.

complex enzyme extraction and purification steps as well as maintaining the activity and stability of intracellular enzymes. Therefore, a lot of chemicals with high-value had been produced by whole cell biocatalysis [13,14] and researches on the production of acetoin by whole-cell biocatalysis had attracted a lot of interest. At present, acetoin with high yield was mainly synthesized from 2,3-butanediol or acetaldehyde. Yamada-Onodera et al. [15] constructed a recombinant *E. coli* HB101 overexpressing glycerol dehydrogenase, which could produce acetoin from 2,3-butanediol with a high enantionmeric excess (*ee*) value of over 99.9%. A new biocatalysis of *E. coli*/pET-*mbdh-nox-vgb* was explored that could synthesize chiral (3*R*)-acetoin from *meso*-2,3-butanediol. Under optimized conditions, 86.74 $g \cdot L^{-1}$ of (3*R*)-acetoin was achieved from 93.73 $g \cdot L^{-1}$ *meso*-2,3-butanediol with a yield of 0.925 $g \cdot g^{-1}$, a productivity of 3.61 $g \cdot L^{-1} \cdot h^{-1}$ and an *ee* value of 95.78% [5]. Bao et al. [16] proposed a strategy of constructing an NAD^+ (nicotinamide adenine dinucleotide) regeneration system for efficiently converting 2,3-butanediol to acetoin by using engineered *B. subtilis* as whole-cell biocatalysis and efficiently produced 91.8 $g \cdot L^{-1}$ of acetoin with a yield and productivity of 0.765 $g \cdot g^{-1}$ and 2.3 $g \cdot L^{-1} \cdot h^{-1}$, respectively. In addition, Zhou et al. [17] used *Gluconobacter oxydans* NL71 for bio-oxidization of 2,3-butanediol to acetoin and 165.9 $g \cdot L^{-1}$ of acetoin was obtained with a yield and productivity of 0.932 $g \cdot g^{-1}$ and 11.43 $g \cdot L^{-1} \cdot h^{-1}$ respectively in 36 h. The highest titer (222 $g \cdot L^{-1}$) of acetoin was produced from acetaldehyde by an *E. coli* whole-cell biocatalytic system [18]. However, both 2,3-butanediol and acetaldehyde are mainly coming from non-renewable fossil resources, the use of fossil fuels might cause the aggravation of environmental pollution and the shortage of fossil resources [3]. Moreover, 2,3-butanediol and acetaldehyde are relative expensive compared to other substrates such as pyruvate and lactate. It is crucial to find a cheap and renewable substrate to produce acetoin efficiently.

Pyruvate, which can be synthesized renewably, is an important molecule in both chemical and biological synthesis process [19–21]. It is the precursor of acetoin that could be obtained by catalysis of α-acetolactate synthetase (ALS) and α-acetolactate decarboxylase (ALDC). *In vitro* enzyme biocatalysis was used to transform pyruvate to acetoin, and 186.7 $g \cdot L^{-1}$ (3*R*)-acetoin was obtained by employing a two-enzyme system composed of ALS and ALDC, which demonstrated a tremendous potential of the acetoin production from pyruvate [19]. However, the high cost of enzyme preparation and short life of enzymes limited the further application in industrial production. Hence, developing an efficient and economic process for high-yield acetoin production from pyruvate is desirable.

Halomonas bluephagenesis TD01, known as the chassis strain of the next-generation of industrial biotechnology, can grow over a wide range of salt concentrations at alkali pH due to their unique characteristics of halophilic microorganisms [22,23]. Compared with other chassis strains, *H. bluephagenesis* has the characteristics of strong robustness and fast growth under the condition of high salinity and alkali pH, and most industrial producers cannot grow under the same condition. Therefore its cultivation is not easy to be contaminated by other microorganisms and it can be cultivated in unsterile continuous biotechnological process, which could greatly simplify operation process and decrease the production cost [22,24–26]. Additionally, with the development of gene editing technology and the research on the metabolic network of halophiles, the high-efficiency and abundant synthesis of important chemicals including polyhydroxyalkanoates [27–29], proteins [30] and chemicals (ectoine [31], 5-aminolevulinic acid [32], 3-hydroxypropionate [33], L-threonine [34], itaconic acid [35], etc.) had been achieved by manipulated halophiles. Moreover, the results of previous substrate profiling and tolerance testing on *H. bluephagenesis* indicated that this chassis strain showed a distinct advantage in utilizing organic acid salts [36]. Hence, *H. bluephagenesis* is a kind of strong chassis strain for industrial application and might utilize pyruvate greatly.

To investigate the feasibility of a new-type *H. bluephagenesis* whole-cell biocatalysis for acetoin production, an efficient whole-cell bioconversion system was constructed for production of acetoin with *H. bluephagenesis* in this work. In the bioconversion system, pyruvate is converted into acetoin by recombinant *H. bluephagenesis* strains expressing ALS and ALDC. Different means of expression of ALS and ALDC were investigated, and conditions were optimized for efficient acetoin production. Furthermore, acetoin productivity was enhanced significantly by increasing the expression of ALS and ALDC. Ultimately, the recombinant *H. bluephagenesis* strain produced 974.3 $mmol \cdot L^{-1}$ of acetoin from 2143.4 $mmol \cdot L^{-1}$ of pyruvate in 8 h, with a promising yield of 0.455 $mol \cdot mol^{-1}$ and a productivity of 10.72 $g \cdot L^{-1} \cdot h^{-1}$. Thus, an economically feasible, efficient and competitive acetoin production bioprocess was established.

2 Experimental

2.1 Strains, chemicals and culture conditions

All strains used in this study are listed in Table 1. *H. bluephagenesis* TD01 is a kind of halophilic bacterium, which is isolated from Aydingkol Lake of China [23]. *H. bluephagenesis* TD1.0 is derived from *H. bluephagenesis* TD01 which has a T7-like expression system that is expressed under the lacI-controlled promotor P_{tac} and induced by isopropyl β-D-thiogalactoside (IPTG) [37]. All

Table 1 Stains and plasmids used in this study

Strains or plasmids	Description	Ref./source
Strains		
E. coli DH5α	Host for plasmid construction	Lab stock
E. coli S17-1 pir	A vector dononr for conjugation experiment harboring tra genes from plasmid RP4 in the chromosome	[38]
H. bluephagenesis TD01	Wild-type *H. bluephagenesis* strain isolated from Aydingkol Lake in Xinjiang Province, China	[39]
TD1.0	*H. bluephagenesis* TD01 with chromosomal integration of T7-like induced system for inducible expression of target genes	[37]
TD1.0Δ*phaC*	*H. bluephagenesis* TD1.0 with the deletion of *phaC* gene encoding PHA synthesis	[40]
TDZ-1	*H. bluephagenesis* TD1.0 harboring plasmid pN59-Mmp1-ALDC-ALS	This study
TDZ-2	*H. bluephagenesis* TD1.0Δ*phaC* harboring plasmid pN59-Mmp1-ALDC-ALS	This study
TDZ-3	*H. bluephagenesis* TD1.0 harboring plasmid pN59-Mmp1-ALDC-S_2-ALS	This study
TDZ-4	*H. bluephagenesis* TD1.0Δ*phaC* harboring plasmid pN59-Mmp1-ALDC-S_2-ALS	This study
TDZ-5	*H. bluephagenesis* TD1.0Δ*phaC* harboring plasmid pN59-Mmp1-ALDC-S_2-ALS and pN85-Mmp1-ALDC	This study
Plasmids		
pN85	A medium copy number expression vector in *H. bluephagenesis* TD strain, Km^R&Sp^R, RK2 replication origin, oriT	[41]
pN59	A high copy number expression vector in *H. bluephagenesis* TD strain, Cm^R. ColE1 replication origin, oriT	[41]
pN59-pct	A high copy number expression vector in *H. bluephagenesis* TD strain, Cm^R. ColE1 replication origin, oriT	[41]
pN59-Mmp1-MCS	pN59 derivates, containing a T7-like inducible promoter, Cm^R	This study
pN59-Mmp1-ALDC-ALS	pN59 derivates, containing *alsD-alsS* fusion gene driven by P_{Mmp1}, Cm^R	This study
pN59-Mmp1-ALDC-S_2-ALS	pN59 derivates, containing *alsD*-linker(10aa)-*alsS* fusion gene driven by P_{Mmp1}, Cm^R	This study
pN85-Mmp1-ALDC	pN85 derivates, containing *alsD* gene driven by P_{Mmp1}, Km^R&Sp^R	This study

engineered strains in this study were derived from *H. bluephagenesis* TD1.0. *E. coli* DH5α was used as host strain for plasmids construction. *E. coli* S17-1 was used as donor strain for plasmids conjugation of *H. bluephagenesis*.

Sodium pyruvate, magnesium chloride and other chemicals were all obtained from Sangon (Sangon Biotech, Shanghai, China), unless stated otherwise. In this study, *E. coli* DH5α and *E. coli* S17-1 were cultured in LB medium (10 $g \cdot L^{-1}$ tryptone, 5 $g \cdot L^{-1}$ yeast extract and 10 $g \cdot L^{-1}$ NaCl). *H. bluephagenesis* and its derivatives for molecular modification and seed were cultured in 60 LB medium (10 $g \cdot L^{-1}$ tryptone, 5 $g \cdot L^{-1}$ yeast extract and 60 $g \cdot L^{-1}$ NaCl, pH adjusted to 9.0 via 5 $mol \cdot L^{-1}$ NaOH). Antibiotics were added when necessary as following concentrations: 50 $\mu g \cdot mL^{-1}$ of kanamycin, 25 $\mu g \cdot mL^{-1}$ of chloramphenicol, 100 $\mu g \cdot mL^{-1}$ of spectinomycin.

2.2 Plasmid construction

All the plasmids constructed in this study were listed in Table 1. Plasmids pN59 and pN85 were used for gene expression in strains [41]. All relevant primers using in plasmids construction were listed in Table S1 (cf. Electronic Supplementary Material, ESM). The genes *alsS* and *alsD* were obtained from *B. subtilis*. The fusion genes *alsD-alsS* and *alsD-linker(10aa)-alsS* were obtained by fusing *alsS* and *alsD* without or with a linker. The sequences of fusion genes were stated in Table S2 (cf. ESM). The fragment pN59, which was used for enzyme expression, was amplified by the primers pN59-F/R. The DNA fragment of promoter P_{Mmp1} was amplified by polymerase chain reaction (PCR) from the plasmid pN59-pct using the primers Mmp1-F/R. Then the two fragments forementioned were fused by circular polymerase extension cloning (CPEC), resulting in the plasmid pN59-Mmp1-MCS. The DNA fragments of *alsD-alsS* encoding ALDC and ALS were amplified by PCR from the genome of *B. subtilis* using the primers DS-F/R. The fragment of pN59-Mmp1-MCS was amplified by the primers pN59-M-F/R. All the fragments were digested with *BamH*I/*Sda*I and assembled to obtain pN59-Mmp1-ALDC-ALS and pN59-Mmp1-ALDC-S_2-ALS respectively. Likewise, the fragment P_{Mmp1}-*alsD* encoding ALDC driven by promoter P_{Mmp1} was amplified by PCR from the plasmid pN59-Mmp1-ALDC-ALS using the primers D-F/R and assembled with the fragment of pN85 amplified by the primers pN85-F/R using CPEC, obtaining the plasmid pN85-Mmp1-ALDC.

2.3 Plasmid conjugation

The plasmid conjugation was conducted according to a previously reported method [23]. Briefly, *E. coli* S17-1 served as the donor strain containing target plasmids was cultured in LB medium with corresponding antibiotics, while the recipient strains were cultured in 60 LB medium. After overnight cultivation, the culture of the donor and recipient cells were collected by centrifuged with the speed of 4500 ×*g* at 4 °C, and washed twice using fresh culture medium, then the cells were mixed (1:1 vol) and spread on 20 LB agar plate and incubated at 37 °C for 8–12 h. At last, the mixed cells were re-suspended by fresh 60 LB medium and spread on 60 LB

agar plate with relevant antibiotics, then incubated at 37 °C for 24–48 h and correct single colonies were selected.

2.4 Preparation of whole-cell biocatalysis

Firstly, the engineered strains were cultured in 5 mL 60 LB medium containing appropriate antibiotics at 37 °C, 220 r·min^{-1} overnight. Secondly, the seed solution was transferred with 1% inoculum to 1 L shake flasks which contained 200 mL 60 LB medium with relevant antibiotics and cultured at 37 °C, 220 r·min^{-1}. After the optical density (OD_{600}) reached to 0.6–0.8, 0.5 mmol·L^{-1} IPTG was added and the temperature was adjusted to 30 °C to induce the expression of the enzymes for 12–14 h. Finally, the cells were harvested by centrifuged with the speed of 5000 ×*g* at 4 °C, and washed by 100 mmol·L^{-1} sodium phosphate buffer containing 60 g·L^{-1} NaCl (60 phosphate buffer (PB), pH 9.0). The cells were re-suspended to a high cell density of 20 OD_{600} by the same buffer to obtain the whole-cell biocatalysis. Cell dry weight (CDW, g·L^{-1}) of *H. bluephagenesis* was calculated from OD_{600} values using the experimentally determined correlation factor of 0.54 g of cells (dry weight [DW])/ liter for an OD_{600} of 1.

2.5 Production of acetoin by whole-cell biocatalysis system

The whole-cell bioconversion was carried out in a 25 mL bottle with a total of 10 mL reaction mixture initially containing about 400 mmol·L^{-1} sodium pyruvate, 0.4 mmol·L^{-1} thiamine pyrophosphate (TPP), 10 mmol·L^{-1} $MgCl_2$, and 100 mmol·L^{-1} 60 PB. Therein, TPP and Mg^{2+} were necessary cofactors bound with ALS. The components were added into the bottle one by one. The collected cells were next added to obtain an initial OD_{600} around 5 and then the reaction was activated. The reaction was displayed at 37 °C and stirred at 220 r·min^{-1}. The reaction mixture (100 μL) were taken and added into 900 μL of 5 mmol·L^{-1} H_2SO_4. Then it was centrifuged with the speed of 12000 ×*g* and the supernatant were taken as samples to measure the concentration of pyruvate, acetoin and by-products.

To achieve a higher yield of acetoin, the effects of the reaction temperature (30, 35, 37, 40, 45, and 50 °C), concentration of Mg^{2+} (0, 5, 10, 15, and 20 mmol·L^{-1}), shaking speed (100, 150, and 220 r·min^{-1}), pH value (6.0, 7.0, 8.0, and 9.0), initial cell density (2.7, 5.4, 8.1, and 10.8 g·L^{-1} cells (DW)) and concentration of pyruvate (400, 800, and 1200 mmol·L^{-1}) were investigated successively.

2.6 Fed-batch biotransformation of acetoin production

Fed-batch biotransformation was carried out in a 25 mL bottle with 10 mL reaction mixture at 45 °C, 220 r·min^{-1}. The pH of reaction cultures was adjusted to 6 every two hours for four times. The initial concentration of pyruvate was about 800 mmol·L^{-1} and 5.4 g·L^{-1} cells (DW) were used for the biotransformation. To improve the efficiency of biocatalysis, a mixture of pyruvic acid and sodium pyruvate or pyruvic acid were fed to adjust the pH of the bio-reaction system to 6.0–6.5 coupling with supplementing the substrate. Samples were taken before and after adjusting pH to measure the concentrations of pyruvate, acetoin and by-products.

2.7 Recycling and reutilization of whole-cell biocatalysis on acetoin production

Recycling and reutilization of whole-cell biocatalysis was carried out in a 25 mL bottle with 10 mL reaction mixture at 45 °C, 220 r·min^{-1}. The pH of reaction culture was adjusted to around 6 and 5.4 g·L^{-1} cells (DW) was added to the reaction system. The culture was centrifuged and the cells were harvested by centrifuged with the speed of 5000 ×*g* at 4 °C, and then the cell was washed by 100 mmol·L^{-1} sodium phosphate buffer containing 60 g·L^{-1} NaCl (60 PB, pH 9.0) every 12 h. Samples were taken after each cycle to measure the concentrations of pyruvate, acetoin and by-products.

2.8 Analytical methods

The biomass was represented by a spectrophotometer at 600 nm. The concentrations of pyruvate, acetoin and by-products were detected via a high-performance liquid chromatography system which was equipped with an HPX-87H (300 mm × 7.8 mm) column (Bio-Rad, Shanghai, China). The detailed information of HPLC measuring method was shown in Fig. S1 (cf. ESM) and Table S3 (cf. ESM). The samples were prepared by filtering through the 0.22 μm syringe filters. The analysis was carried out at 60 °C with a mobile phase of 5 mmol·L^{-1} H_2SO_4 at a flow rate of 0.5 mL·min^{-1}. The theoretical yield was 0.5 mol acetoin/mol pyruvate.

3 Results and discussion

3.1 Feasibility of acetoin production from pyruvate by whole-cell biocatalysis

H. bluephagenesis TD01, a chassis strain with a resistance of alkali conditions, has been proved that it had prominent tolerability to organic acid, such as itaconic acid, succinic acid [36]. Therefore, it was rational to propose that *H. bluephagenesis* TD01 could have good tolerance of pyruvate and use pyruvate efficiently. However, the metabolite detection and gene sequence

analysis indicated that there was no acetoin synthesis pathway in *H. bluephagenesis*, which meant acetoin could not be synthesized naturally. Thus, the acetoin synthesis pathway should be introduced heterogeneously into *H. bluephagenesis*.

The pathway from pyruvate to acetoin includes a two-step reaction process catalyzed by ALS and ALDC (Fig. 1). ALS and ALDC from *B. subtilis* (*bsu*-ALS and *bsu*-ALDC, respectively) were chosen due to their good performance in acetoin production in our previous study [10,19]. *bsu*-ALS and *bsu*-ALDC were fused in different ways and overexpressed in *H. bluephagenesis* through high copy plasmid pN59 to produce acetoin efficiently. Hence, the engineered strains TDZ-1 to TDZ-4 (Table 1) expressing the fusion enzymes were constructed using strains TD1.0 or TD1.0Δ*phaC* as hosts. Subsequently, the abilities of the engineered strains catalyzing approximately 400 mmol·L^{-1} pyruvate to produce acetoin were detected. TDZ-1 to TDZ-4 could utilize the pyruvate completely within 36 h and the pyruvate consumption rate showed nearly no difference. Among the four engineered strains, TDZ-4 could synthesis 125.4 mmol·L^{-1} acetoin in 36 h, which showed higher catalytic activity with a yield of 0.333 mol·mol^{-1} and a productivity of 3.484 mmol·L^{-1}·h^{-1} (Fig. 2). Moreover, different hosts also had different influence on the catalytic ability to some extent. By employing the TD1.0 chassis, TDZ-1 and TDZ-2 with different fusion types showed similar performance of acetoin production. However, the engineered strains TDZ-3 and TDZ-4, derived from TD1.0Δ*phaC* chassis, both exhibited higher acetoin concentration. Significantly, the S_2 linker fusion type and blocking PHB synthesis in TDZ-4, showed synergistic effect on enhanced acetoin production. As shown in Fig. 2, TDZ-4 afforded much higher acetoin yield and productivity, which might be caused by the

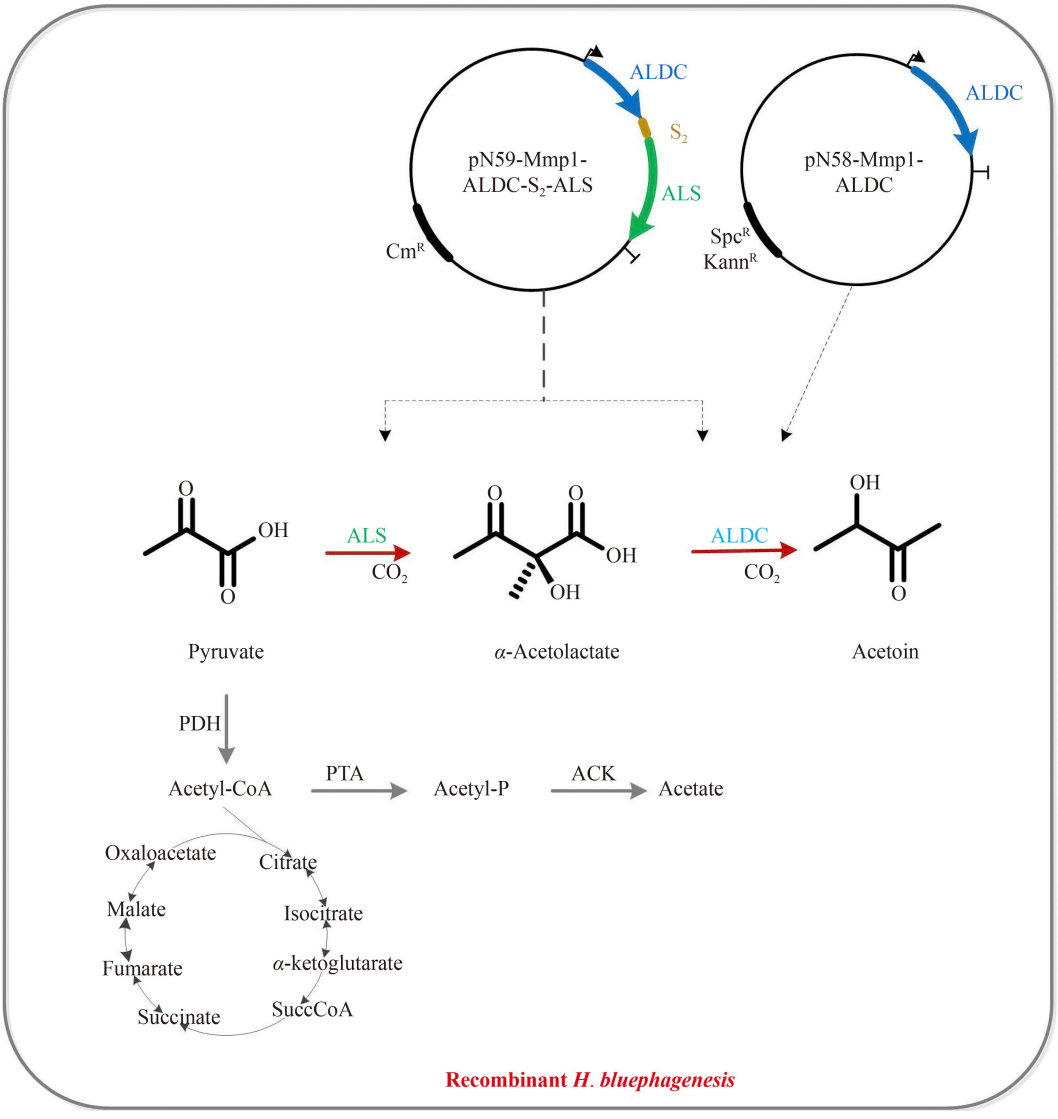

Fig. 1 Scheme of acetoin production from pyruvate catalyzed by *H. bluephagenesis* (PDH, pyruvate dehydrogenase complex; PTA, phosphate acetyltransferase; ACK, acetate kinase).

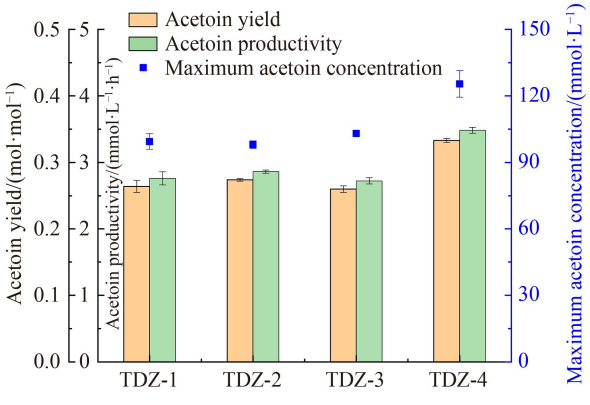

Fig. 2 Acetoin yield, acetoin productivity and maximum acetoin concentration of engineered strains TDZ-1 to TDZ-4 (Error bars represent the standard deviation of triplicate experiments).

highly efficient catalysis with S_2 linker and blocking the PHB synthesis pathway to save more pyruvate for acetoin synthesis. However, pyruvate was not completely transformed into acetoin, which might be caused by the unbalanced flux through the acetoin synthetic pathway. Thus, optimization of reaction conditions could be an efficient method to improve conversion rate of *α*-acetolactate to acetoin.

3.2 Optimization of bioconversion conditions for acetoin production from pyruvate

For the purpose of improving the efficiency of whole-cell biocatalysis to obtain higher acetoin yield, a series of reaction conditions were optimized with TDZ-4 (Fig. 3) which had higher catalytic capacity.

Firstly, the effect of reaction temperature on whole-cell biocatalysis was studied in the range of 30–50 °C. The results displayed that pyruvate was completely consumed at different temperatures within 36 h and the pyruvate consumption rate increased along with the increase of temperature (Fig. 3(a)). Moreover, the highest acetoin titer of 140.2 mmol·L^{-1} was obtained from 394.9 mmol·L^{-1} pyruvate at 45 °C in 30 h, and the acetoin yield and productivity were 0.355 mol·mol^{-1} and 4.67 mmol·L^{-1}·h^{-1}, respectively (Fig. 3(b)). The optimization of Mg^{2+} concentration could enhance the ability of ALS thus improved the production of acetoin. Then the effect of Mg^{2+} concentration was investigated. Different concentrations of Mg^{2+} from 0 to 20 mmol·L^{-1} were set to test their effects on acetoin production. The increase of Mg^{2+} concentration showed positive effect on pyruvate consumption (Fig. 3(c)), but it had little negative effect on acetoin production (Fig. 3(d)). As a result, the production of acetoin reached 167.7 from 436.7 mmol·L^{-1} pyruvate and the highest yield and productivity of acetoin (0.384 mol·mol^{-1} and 5.41 mmol·L^{-1}·h^{-1}, respectively) were obtained at 45 °C without Mg^{2+} addition after 30 h cultivation. Meanwhile, since the rotational speed was related to the catalytic stability and activity of strains, the effect of rotational speed was detected. However, the influence of different rotational speeds did not display distinct difference (Fig. S2, cf. ESM). Considering that the catalysis conditions with higher cell density and substrate concentration would be tested in subsequent experiments, the rotational speed was set to 220 r·min^{-1} in the following study.

The effect of pH on the whole-cell biocatalysis was investigated due to its potential influence on enzyme activities. The result indicated that the production of acetoin decreased with the increase of initial pH. The highest titer of acetoin reached 204.3 from 476.2 mmol·L^{-1} pyruvate when the initial pH was set to 6.0 (Fig. 3(e)). However, pyruvate consumption rate was not affected by different initial pH (data not shown). The acetoin yield and productivity were 0.429 mol·mol^{-1} and 7.46 mmol·L^{-1}·h^{-1}, respectively, after 24 h cultivation. Therefore, the optimal initial pH value of 6.0 was used in the following experiments. It had been reported that the optimal initial pH was 6.0 that is the optimal pH for ALDC activity [19]. The pyruvate consumption rate and acetoin production rate were very fast, and pH rose to alkalinity rapidly (data not shown). Moreover, the system would remain in alkalinity for a long time, and *H. bluephagenesis* that has good tolerance to alkaline environment could be more adaptable to the catalytic environment than other organisms such as *E. coli*.

Finally, the influence of cell density was surveyed owing to its significant effect on the efficiency of product formation rate. Unexpectedly, the acetoin productivity didn't increase with the increase of the cell density, and the highest titer of acetoin reached 197.2 from 454.4 mmol·L^{-1} pyruvate with the highest productivity and yield of acetoin (8.10 mmol·L^{-1}·h^{-1} and 0.434 mol·mol^{-1}, respectively) when the initial cell was 5.4 g·L^{-1} (Fig. 3(f)). However, the pyruvate consumption rate obviously improved with the increase of cell density, and the acetoin formation was almost ceased at 12 h when the cells was 8.1 or 10.8 g·L^{-1} (DW) (Fig. S3, cf. ESM). We speculated that the intermediate product *α*-acetolactate could be accumulated to a much high level under the condition of higher cell density, which exerted a negative effect on cell activity. Therefore, the optimal conditions for acetoin production were 45 °C, pH 6.0, 220 r·min^{-1} and 5.4 g·L^{-1} cells.

3.3 Further increase of ALDC expression for efficient acetoin production

After a series of optimization, the strain TDZ-4 could almost use the pyruvate up in 6 h with a yield of 85.7% of the theoretical yield. However, the acetoin yield was still not high, and the acetoin titer gradually reached its maximum at 24 h, indicating the acetoin production rate was much slower than pyruvate consumption rate, and the

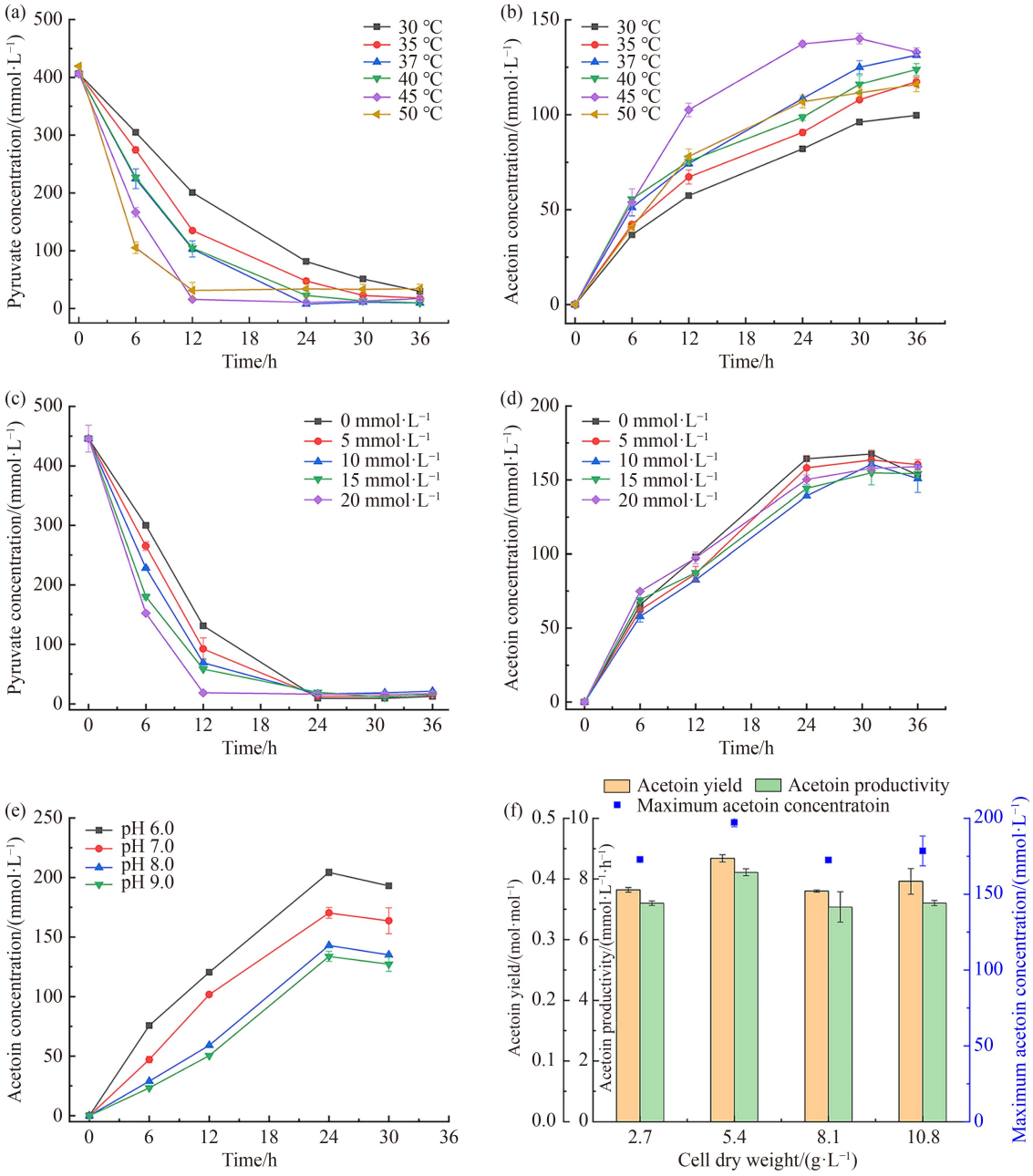

Fig. 3 The process optimization for efficient acetoin biosynthesis using TDZ-4. (a) The effect of temparature on pyruvate consumption; (b) the effect of temparature on acetoin production; (c) the effect of Mg^{2+} concentration on pyruvate consumption; (d) the effect of Mg^{2+} concentration on acetoin production; (e) the effect of pH on acetoin production; (f) the effect of cell dry weight on acetoin yield, acetoin productivity and maximum acetoin concentration (Error bars represent the standard deviation of triplicate experiments).

intermediate product *α*-acetolactate was probably accu mulated. Possibly the second step was the rate-limiting step and the expression of ALDC was insufficient. Thus, it might be necessary to further increase the expression level of ALDC in TDZ-4 to balance the rates of the two reactions.

To enhance the metabolic flux from *α*-acetolactate to acetoin and increase the acetoin productivity, the gene *alsD* was cloned into plasmid pN85 equipped with the promoter P_{Mmp1} to obtain pN85-Mmp1-ALDC. Subse quently, the plasmid pN85-Mmp1-ALDC was conjugated into TDZ-4, generating strain TDZ-5. As shown in Fig. 4, the acetoin concentration of TDZ-5 was rather higher than that of TDZ-4 in 6 h (Fig. 4(a)). Besides, the acetoin yield and productivity of TDZ-5 were 0.491 $mol \cdot mol^{-1}$ and 37.24 $mmol \cdot L^{-1} \cdot h^{-1}$, which increased 14.7% and 359.5% respectively compared with TDZ-4 (Fig. 4(b)). The productivity was significantly improved by overexpressing *alsD*, which indicated the rates of the two reactions catalyzed by ALS and ALDC were well

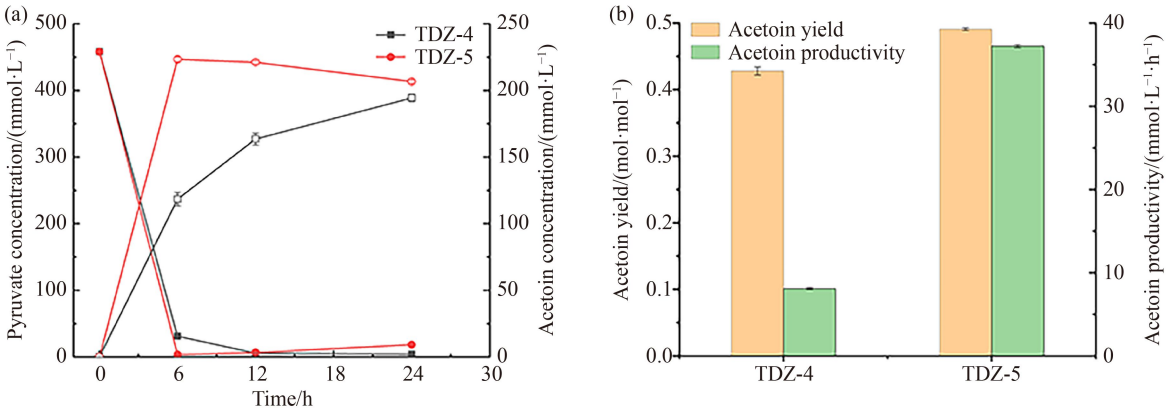

Fig. 4 The profile of pyruvate consumption and acetoin production in whole-cell biocatalysis using TDZ-4 and TDZ-5. (a) Pyruvate consumption and acetoin production of TDZ-4 and TDZ-5; (b) acetoin yield and productivity of TDZ-4 and TDZ-5 (Error bars represent the standard deviation of triplicate experiments).

balanced. Many studies have indicated that coordination of the expression levels or activities of enzymes could improve catalysis efficiency significantly. Wang et al. [42] optimized the expression of 5-aminovaleramide amidohydrolase and L-lysine 2-monooxygenasethe by transforming another plasmid and therefore the yield of this engineered strain was 1.3 fold higher than that of the former strain in the production of 5-aminovalerate from L-lysine. Besides, Zhang et al. [35] increased the itaconic acid titer from 3.38 to 5.70 g·L^{-1} by increasing the expression level of the rate-limiting enzyme cis-aconitase.

3.4 Effect of different pyruvate concentrations on acetoin production

In order to obtain a higher production of acetoin, different pyruvate concentrations in the range of 400 to 1200 mmol·L^{-1} were used in order to get higher acetoin concentration under the optimum conditions (Fig. 5). As shown in Figs. 5(a) and 5(b), the reaction rate was quick in first 2 h, both 400 and 800 mmol·L^{-1} pyruvate can be completely consumed within 2 h, and the time was prolonged to 6 h for 1200 mmol·L^{-1} pyruvate. However, acetoin productivity was decreased sharply as substrate concentration increased over 800 mmol·L^{-1}, and the yield of acetoin dropped obviously with the increase of pyruvate concentration. The pyruvate consumption rates under different pyruvate concentrations in 2 h were 201.7, 400.0 and 281.9 mmol·L^{-1}·h^{-1} and the acetoin synthesis rates were 106.7, 160.2 and 40.6 mmol·L^{-1}·h^{-1}, respectively. The reaction rates indicated that the reaction system still had a high catalytic ability under 800 mmol·L^{-1} pyruvate. The titer of acetoin reached 388.5 mmol·L^{-1} in 2 h and the yield kept at a high level of 0.485 mol·mol^{-1}. The productivity of acetoin reached 199.58 mmol·L^{-1}·h^{-1}, which was much higher compared with other whole-cell biocatalysis [43,44]. During the reaction process, acetate and succinate were accumulated as main by-products and their concentrations were also increased with the increase of pyruvate concentration (Fig. 5(c)). It could be seen that approximately 8.3 mmol·L^{-1} acetate and 39.7 mmol·L^{-1} succinate were accumulated at 24 h when the concentration of pyruvate was 1200 mmol·L^{-1}. The accumulated succinate demonstrated that some pyruvate was directed into the tricarboxylic acid cycle. Moreover, the unstable intermediate product α-acetolactic acid might be extensively accumulated, which resulted in low acetoin yield. Thus, knocking out or weakening by-products synthesis genes would be conducted in future to enhance

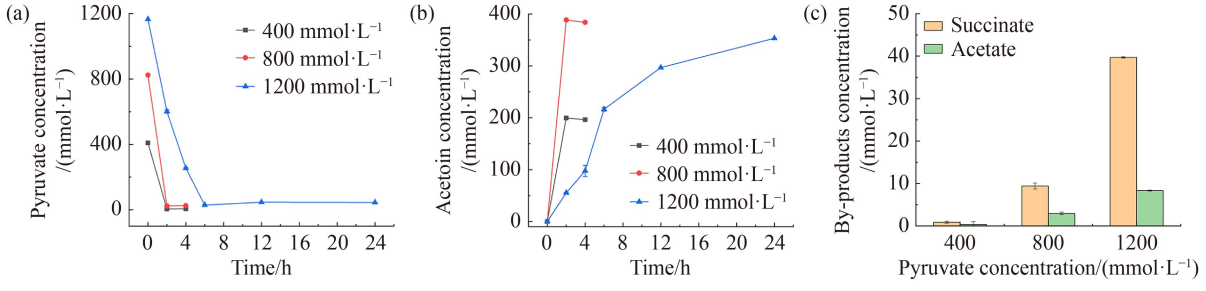

Fig. 5 The profile of pyruvate consumption, acetoin production and by-products synthesis under different pyruvate concentration. (a) The effect of pyruvate concentration on pyruvate consumption; (b) the effect of pyruvate concentration on acetoin production; (c) the concentrations of by-products in reaction system under different pyruvate concentrations (Error bars represent the standard deviation of triplicate experiments).

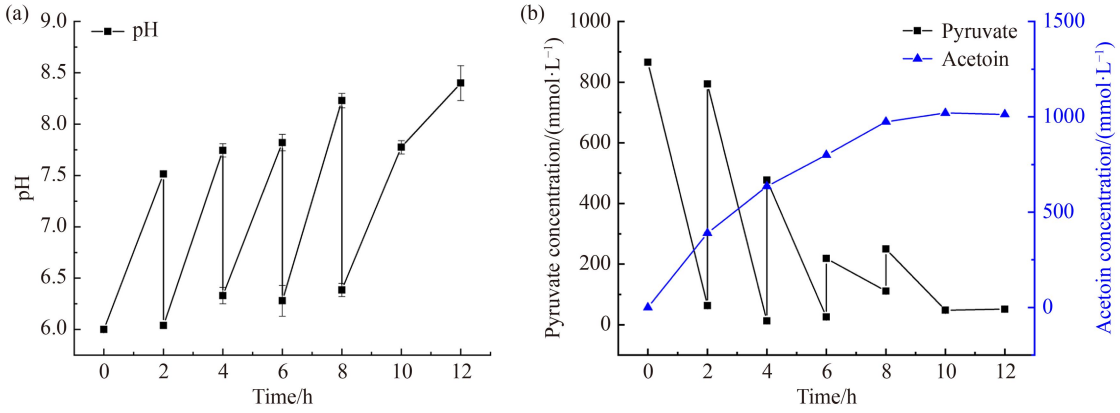

Fig. 6 The time profile of pH and acetoin production in fed-batch using TDZ-5. (a) pH value of the reaction system; (b) pyruvate consumption and acetoin production in fed-batch bioconversion of TDZ-5 (Error bars represent the standard deviation of triplicate experiments).

acetoin production and yield when a high concentration of pyruvate is used. Therefore, the substrate concentration was set as 800 mmol·L^{-1} for subsequent study due to its high acetoin titer, yield and productivity.

3.5 Enhancement of acetoin production in fed-batch catalysis

As it's difficult to increase acetoin titer by further increasing pyruvate concentrations, a fed-batch strategy was adopted to test its effect on acetoin synthesis (Fig. 6). It was found that TDZ-5 could utilize 800 mmol·L^{-1} pyruvate completely in 2 h and the pH of reaction culture increased to around 8.5 rapidly during the catalysis process, which could greatly affect ALS and ALDC activities whose optimal pH were 7.0 and 6.0, respectively [45]. Therefore it was important to adjust pH to maintain enzymes activities. Due to the difficulty of monitoring pH and maintaining constant pH in a small bottle (25 mL), a fed-batch strategy that adding the mixture of pyruvic acid and sodium pyruvate every two hours was used to not only adjust the pH but also provide substrate (Fig. 6(a)). From 0 to 4 h, a mixture of pyruvic acid and sodium pyruvate with a mole ratio of 5:1 was used, and only pyruvic acid was used to adjust the culture pH after 4 h. As shown in Fig. 6(b), a high titer of 974.3 mmol·L^{-1} acetoin was accumulated from 2143.4 mmol·L^{-1} pyruvate after 8 h cultivation, and the acetoin yield and productivity were 0.454 mol·mol^{-1} and 121.79 mmol·L^{-1}·h^{-1}, respectively. It was worth noting that the acetoin titer no longer increased and the pyruvate consumption rate also decreased to a relatively low level after 8 h, which meant the strain lost the catalytic ability probably caused by the high concentration of acetoin. We tested the effect of acetoin addition on the performance of whole-cell biocatalysis. As shown in Fig. S4 (cf. ESM), the concentration, yield and productivity of acetoin gradually decreased with the increase of initial acetoin concentration. In our previous study, the acetoin titer

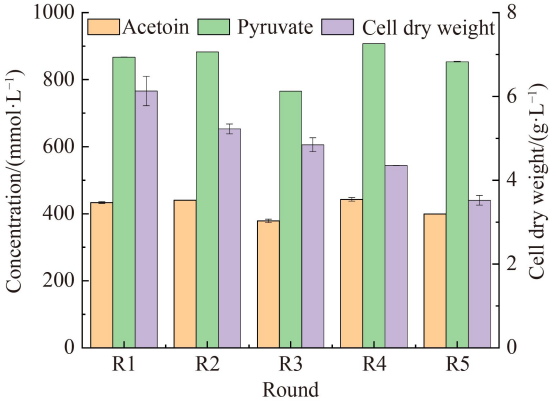

Fig. 7 Acetoin production, acetoin yield and cell dry weight of TDZ-5 in repeated batch bioconversion. The pyruvate addition concentrations were 867.2, 882.6, 765.7, 907.9 and 853.6 mmol·L^{-1}, respectively. Error bars represent the standard deviation of triplicate experiments.

could reach 186.7 g·L^{-1} (2118.9 mmol·L^{-1}) in a two-enzyme cascade composed of ALS and ALDC [19], so it was unlikely that the ALDC was inhibited when the acetoin concentration reached 974.3 mmol·L^{-1} in this fed-batch system. The exact reason for that is still unclear and need to be explored in future study.

3.6 Recycling and reutilization of whole-cell biocatalysis

In order to test the reusability of the biocatalysis, a repeated recycling process of whole-cell catalysis was implemented. As shown in Fig. 7 and Table 2, the acetoin titer was 433.3, 440.2, 379.0, 442.8 and 339.4 mmol·L^{-1} (38.2, 38.8, 33.4, 39.0 and 29.9 g·L^{-1}) from the first to the fifth round of catalysis, respectively. The corresponding acetoin yields were 99.8%, 99.8%, 99%, 97.6% and 93.6% of the theoretical yield. However, the CDW decreased from 6.14 to 2.47 g·L^{-1} after four rounds, and the loss of whole-cell biocatalysis during centrifugation or inoculation might be related to the obviously decrease of the bioconversion efficiency. The efficiency of whole-

Table 2 Recycling and reutilization of biocatalysis

Cycle	Pyruvate concentration/(mmol·L^{-1})	Acetoin concentration/(mmol·L^{-1})	Cell density/OD_{600}	Acetoin yield/(mol·mol^{-1})	Acetoin yield of the theoretical yield/%
1	867.2 ± 0.05	433.3 ± 2.4	11.37 ± 0.37	0.499 ± 0.01	99.8 ± 1.0
2	882.6 ± 0.0	440.2 ± 0.5	8.07 ± 0.04	0.499 ± 0.02	99.8 ± 2.0
3	765.7 ± 0.0	379.0 ± 5.2	5.13 ± 0.14	0.495 ± 0.023	99.0 ± 2.3
4	907.9 ± 0.0	442.8 ± 5.4	4.96 ± 0.09	0.488 ± 0.017	97.6 ± 1.7
5	853.6 ± 1.0	399.4 ± 0.1	4.57 ± 0.28	0.468 ± 0.022	93.6 ± 2.2

cell biocatalysis could be maintained at a high level by cell immobilization, by which the biocatalysis could be separated easily from reaction system and reused in repeated or continuous process [46].

A highest acetoin titer of 186.7 from 395.6 g·L^{-1} pyruvate *in vitro* with 94.3% theoretical yield and a productivity of 15.56 g·L^{-1}·h^{-1} was obtained in our previous study [19]. And the highest titer of acetoin by microbial fermentation reached 102.45 g·L^{-1} with a yield of 0.419 g·g^{-1} glucose and a productivity of 1.86 g·L^{-1}·h^{-1} [10]. Although the titer obtained here was not the highest, this acetoin production process eliminated enzyme extraction and purification steps which reduced production cost, and enzyme activity could be remained for longer time than that of *in vitro*. Compared to the microbial fermentation, whole-cell biocatalysis using *H. bluephagenesis* had advantages of high acetoin production rate and simplified downstream separation process. Due to the relatively simple composition of the supernatant after reaction compared to fermentation broth, it is beneficial to acetoin separation in the downstream. Salting-out extraction methods using acetone/K_2HPO_4 [47], ethanol/K_3PO_4 or ethyl acetate/K_2HPO_4 [48] could be applied for extraction of acetoin. After the extraction, acetoin could be further recovered and concentrated through rotary evaporation.

The acetoin production in our work was not the highest compared to other whole-cell biocatalysis using 2,3-butanediol or acetaldehyde as substrates. However, the cell density used in this catalysis route was very low, and the pyruvate was relatively cheap and renewable which could be produced with a titer of over 100 g·L^{-1} by fermentation from other renewable and cheap resources [49]. In addition, the fermentation broth of pyruvate can be directly used in this whole-cell biocatalysis process to further decrease production cost. The result of this study demonstrated the potential of whole-cell biocatalysis for the bio-production of acetoin from pyruvate using recombinant *H. bluephagenesis*.

4 Conclusions

In conclusion, an effective *H. bluephagenesis* whole-cell bioconversion system was developed for acetoin production from pyruvate. The engineered strains were constructed using different plasmids to co-express ALS and ALDC from *B. subtilis* 168 which exhibited high efficiency of utilizing pyruvate to synthesize acetoin. After a series of conditions optimization and further increase of ALDC expression, 223.4 mmol·L^{-1} of acetoin was obtained from 458.1 mmol·L^{-1} of pyruvate with a yield of 0.491 mol·mol^{-1} and a productivity of 37.24 mmol·L^{-1}·h^{-1} in 6 h. Finally, 974.3 mmol·L^{-1} (85.84 g·L^{-1}) of acetoin was accumulated from 2143.4 mmol·L^{-1} (188.6 g·L^{-1}) of pyruvate in 8 h with 90.8% theoretical yield and a productivity of 121.79 mmol·L^{-1}·h^{-1} (10.73 g·L^{-1}·h^{-1}) in fed-batch bioconversion, and 433.3, 440.2, 379.0, 442.8 and 339.4 mmol·L^{-1} (38.2, 38.8, 33.4, 39.0 and 29.9 g·L^{-1}) acetoin were produced respectively in the five batch of repeated cycling process. To the best of our knowledge, this is the first report on acetoin production from pyruvate by *H. bluephagenesis* whole-cell biocatalysis. The results in this work demonstrated that the recombinant *H. bluephagenesis* had great potential to produce a high concentration of acetoin and a promise of economically industrial acetoin bio-manufacturing.

Acknowledgements This work was supported by the National Key Research and Development Program of China (Grant No. 2018YFA0900200) and the National Natural Science Foundation of China (Grant No. NSFC-21621004). We thank Prof. Guo-Qiang Chen from Tsinghua University for generously providing experimental materials.

Electronic Supplementary Material Supplementary material is available in the online version of this article at https://dx.doi.org/10.1007/s11705-022-2229-0 and is accessible for authorized users.

References

1. Xiao Z, Xu P. Acetoin metabolism in bacteria. Critical Reviews in Microbiology, 2007, 33(2): 127–140
2. Wang M, Fu J, Zhang X, Chen T. Metabolic engineering of *Bacillus subtilis* for enhanced production of acetoin. Biotechnology Letters, 2012, 34(10): 1877–1885
3. Xu H, Cui Y, Tian Y, Wang S, Zhu K, Zhou S, Huang Y, He Q, Han Y, Liu L, Li W, Zhu L, Jiang G, Liu J. A summary of producing acetoin by biological method. World Journal of Food Science and Technology, 2020, 4(4): 90–103
4. Sun J A, Zhang L Y, Rao B, Shen Y L, Wei D Z. Enhanced acetoin production by *Serratia marcescens* H32 with expression of a water-forming NADH oxidase. Bioresource Technology, 2012, 119: 94–98

5. He Y Z, Chen F X, Sun M J, Gao H F, Guo Z W, Lin H, Chen J B, Jin W S, Yang Y L, Zhang L Y, Yuan J. Efficient (3*S*)-acetoin and (2*S*,3*S*)-2,3-butanediol production from *meso*-2,3-butanediol using whole-cell biocatalysis. Molecules, 2018, 23(3): 691
6. Cui Z Z, Wang Z W, Zheng M Y, Chen T. Advances in biological production of acetoin: a comprehensive overview. Critical Reviews in Biotechnology, 2021, in press
7. Maina S, Prabhu A A, Vivek N, Vlysidis A, Koutinas A, Kumar V. Prospects on bio-based 2,3-butanediol and acetoin production: recent progress and advances. Biotechnology Advances, 2021, 54: 107783
8. Xu H, Jia S R, Liu J J. Development of a mutant strain of *Bacillus subtilis* showing enhanced production of acetoin. African Journal of Biotechnology, 2011, 10(5): 779–788
9. Bae S J, Kim S, Hahn J S. Efficient production of acetoin in *Saccharomyces cerevisiae* by disruption of 2,3-butanediol dehydrogenase and expression of NADH oxidase. Scientific Reports, 2016, 6(1): 1–8
10. Lu L X, Mao Y F, Kou M Y, Cui Z Z, Jin B, Chang Z S, Wang Z W, Ma H W, Chen T. Engineering central pathways for industrial-level (3*R*)-acetoin biosynthesis in *Corynebacterium glutamicum*. Microbial Cell Factories, 2020, 19(1): 102
11. Bae S J, Kim S, Park H J, Kim J, Jin H, Kim B G, Hahn J S. High-yield production of (*R*)-acetoin in *Saccharomyces cerevisiae* by deleting genes for NAD(P)H-dependent ketone reductases producing *meso*-2,3-butanediol and 2,3-dimethylglycerate. Metabolic Engineering, 2021, 66: 68–78
12. Almuharef I, Rahman M S, Qin W. Enzymatic conversion of glycerol to 2,3-butanediol and acetoin by *Serratia proteamaculans* SRWQ1. Waste and Biomass Valorization, 2018, 10(7): 1833–1844
13. Wachtmeister J, Rother D. Recent advances in whole cell biocatalysis techniques bridging from investigative to industrial scale. Chemical biotechnology, 2016, 42: 169–177
14. Fukuda H, Hama S, Tamalampudi S, Noda H. Whole-cell biocatalysts for biodiesel fuel production. Trends in Biotechnology, 2008, 26(12): 668–673
15. Yamada-Onodera K, Yamamoto H, Kawahara N, Tani Y. Expression of the gene of glycerol dehydrogenase from *Hansenula polymorpha* Dl-1 in *Escherichia coli* for the production of chiral compounds. Acta Biotechnologica, 2002, 22(3–4): 355–362
16. Bao T, Zhang X, Rao Z, Zhao X J, Zhang R Z, Yang T W, Xu Z H, Yang S T. Efficient whole-cell biocatalyst for acetoin production with NAD^+ regeneration system through Homologous co-expression of 2,3-butanediol dehydrogenase and NADH oxidase in engineered *Bacillus subtilis*. PLoS One, 2014, 9(7): e102951
17. Zhou X L, Zhou X, Zhang H Y, Cao R, Xu Y. Improving the performance of cell biocatalysis and the productivity of acetoin from 2,3-butanediol using a compressed oxygen supply. Process Biochemistry, 2018, 64: 46–50
18. Peng K, Guo D, Lou Q, Lu X, Cheng J, Qiao J, Lu L, Cai T, Liu Y, Jiang H. Synthesis of ligustrazine from acetaldehyde by a combined biological-chemical approach. ACS Synthetic Biology, 2020, 9(11): 2902–2908
19. Cui Z Z, Mao Y F, Zhao Y J, Zheng M Y, Wang Z W, Ma H W, Chen T. One-pot efficient biosynthesis of (3*R*)-acetoin from pyruvate by a two-enzyme cascade. Catalysis Science & Technology, 2020, 10(22): 7734–7744
20. Jia X, Liu Y, Han Y. A thermophilic cell-free cascade enzymatic reaction for acetoin synthesis from pyruvate. Scientific Reports, 2017, 7(1): 1–10
21. Pundir C S, Malik M, Chaudhary R. Quantification of pyruvate with special emphasis on biosensors: a review. Microchemical Journal, 2019, 146: 1102–1112
22. Chen G Q, Jiang X R. Next generation industrial biotechnology based on extremophilic bacteria. Current Opinion in Biotechnology, 2018, 50: 94–100
23. Tan D, Wu Q, Chen J C, Chen G Q. Engineering *Halomonas* TD01 for the low-cost production of polyhydroxyalkanoates. Metabolic Engineering, 2014, 26: 34–47
24. Chen X, Yu L, Qiao G, Chen G Q. Reprogramming *Halomonas* for industrial production of chemicals. Journal of Industrial Microbiology & Biotechnology, 2018, 45(7): 545–554
25. Zhang X, Lin Y, Chen G Q. Halophiles as chassis for bioproduction. Advanced Biosystems, 2018, 2(11): 1800088
26. Yin J, Chen J C, Wu Q, Chen G Q. Halophiles, coming stars for industrial biotechnology. Biotechnology Advances, 2015, 33(7): 1433–1442
27. Ye J, Hu D, Che X, Jiang X, Li T, Chen J, Zhang H M, Chen G Q. Engineering of *Halomonas bluephagenesis* for low cost production of poly(3-hydroxybutyrate-co-4-hydroxybutyrate) from glucose. Metabolic Engineering, 2018, 47: 143–152
28. Ling C, Qiao G Q, Shuai B W, Olavarria K, Yin J, Xiang R J, Song K N, Shen Y H, Guo Y, Chen G Q. Engineering NADH/NAD(+) ratio in *Halomonas bluephagenesis* for enhanced production of polyhydroxyalkanoates (PHA). Metabolic Engineering, 2018, 49: 275–286
29. Chen Y, Chen X Y, Du H T, Zhang X, Ma Y M, Chen J C, Ye J W, Jiang X R, Chen G Q. Chromosome engineering of the TCA cycle in *Halomonas bluephagenesis* for production of copolymers of 3-hydroxybutyrate and 3-hydroxyvalerate (PHBV). Metabolic Engineering, 2019, 54: 69–82
30. Zhao H, Yao Z, Chen X, Wang X, Chen G Q. Modelling of microbial polyhydroxyalkanoate surface binding protein PhaP for rational mutagenesis. Microbial Biotechnology, 2017, 10(6): 1400–1411
31. Ma H, Zhao Y, Huang W, Zhang L, Wu F, Ye J, Chen G Q. Rational flux-tuning of *Halomonas bluephagenesis* for co-production of bioplastic PHB and ectoine. Nature Communications, 2020, 11(1): 1–12
32. Li T, Guo Y Y, Qiao G Q, Chen G Q. Microbial synthesis of 5-aminolevulinic acid and its coproduction with polyhydroxybutyrate. ACS Synthetic Biology, 2016, 5(11): 1264–1274
33. Jiang X R, Yan X, Yu L P, Liu X Y, Chen G Q. Hyperproduction of 3-hydroxypropionate by *Halomonas bluephagenesis*. Nature Communications, 2021, 12(1): 1–13
34. Du H, Zhao Y, Wu F, Ouyang P, Chen J, Jiang X, Ye J, Chen G Q. Engineering *Halomonas bluephagenesis* for L-threonine production. Metabolic Engineering, 2020, 60: 119–127

35. Zhang J, Jin B, Hong K, Lv Y, Wang Z, Chen T. Cell catalysis of citrate to itaconate by engineered *Halomonas bluephagenesis*. ACS Synthetic Biology, 2021, 10(11): 3017–3027
36. Zhang J, Zhang X, Mao Y, Jin B, Guo Y, Wang Z, Chen T. Substrate profiling and tolerance testing of *Halomonas* TD01 suggest its potential application in sustainable manufacturing of chemicals. Journal of Biotechnology, 2020, 316: 1–5
37. Zhao H, Zhang H M, Chen X, Li T, Wu Q, Ouyang Q, Chen G Q. Novel T7-like expression systems used for *Halomonas*. Metabolic Engineering, 2017, 39: 128–140
38. Simon R, Priefer U, Pühler A. A broad host range mobilization system for *in vivo* genetic engineering: transposon mutagenesis in Gram negative bacteria. Bio/Technology, 1983, 1(9): 784–791
39. Tan D, Xue Y S, Aibaidula G, Chen G Q. Unsterile and continuous production of polyhydroxybutyrate by *Halomonas* TD01. Bioresource Technology, 2011, 102(17): 8130–8136
40. Qin Q, Ling C, Zhao Y, Yang T, Yin J, Guo Y, Chen G Q. CRISPR/Cas9 editing genome of extremophile *Halomonas* spp. Metabolic Engineering, 2018, 47: 219–229
41. Silva-Rocha R, Martinez-Garcia E, Calles B, Chavarria M, Arce-Rodriguez A, de Las Heras A, Paez-Espino A D, Durante-Rodriguez G, Kim J, Nikel P I, Platero R, de Lorenzo V. The Standard European Vector Architecture (SEVA): a coherent platform for the analysis and deployment of complex prokaryotic phenotypes. Nucleic Acids Research, 2013, 41(D1): D666–D675
42. Wang X, Cai P P, Chen K Q, Ouyang P K. Efficient production of 5-aminovalerate from L-lysine by engineered *Escherichia coli* whole-cell biocatalysts. Journal of Molecular Catalysis B: Enzymatic, 2016, 134: 115–121
43. Li J X, Huang Y Y, Chen X R, Du Q S, Meng J Z, Xie N Z, Huang R B. Enhanced production of optical (*S*)-acetoin by a recombinant *Escherichia coli* whole-cell biocatalyst with NADH regeneration. RSC Advances, 2018, 8(53): 30512–30519
44. Guo Z, Zhao X, He Y, Yang T, Gao H, Li G, Chen F, Sun M, Lee J K, Zhang L. Efficient (3*R*)-acetoin production from *meso*-2,3-Butanediol using a new whole-cell biocatalyst with co-expression of *meso*-2,3-butanediol dehydrogenase, NADH oxidase, and *Vitreoscilla* Hemoglobin. Journal of Microbiology and Biotechnology, 2017, 27(1): 92–100
45. Cui Z Z, Zhao Y J, Mao Y F, Shi T, Lu L X, Ma H W, Wang Z W, Chen T. *In vitro* biosynthesis of optically pure D-(−)-acetoin from *meso*-2,3-butanediol using 2,3-butanediol dehydrogenase and NADH oxidase. Journal of Chemical Technology and Biotechnology, 2019, 94(8): 2547–2554
46. Zajkoska P, Rebros M, Rosenberg M. Biocatalysis with immobilized *Escherichia coli*. Applied Microbiology and Biotechnology, 2013, 97(4): 1441–1455
47. Sun J, Rao B, Zhang L, Shen Y, Wei D. Extraction of acetoin from fermentation broth using an acetone/phosphate aqueous two-phase system. Chemical Engineering Communications, 2012, 199(11): 1492–1503
48. Dai J, Guan W, Ma L, Xiu Z. Salting-out extraction of acetoin from fermentation broth using ethyl acetate and K_2HPO_4. Separation and Purification Technology, 2017, 184: 275–279
49. Becker J, Lange A, Fabarius J, Wittmann C. Top value platform chemicals: bio-based production of organic acids. Current Opinion in Biotechnology, 2015, 36: 168–175